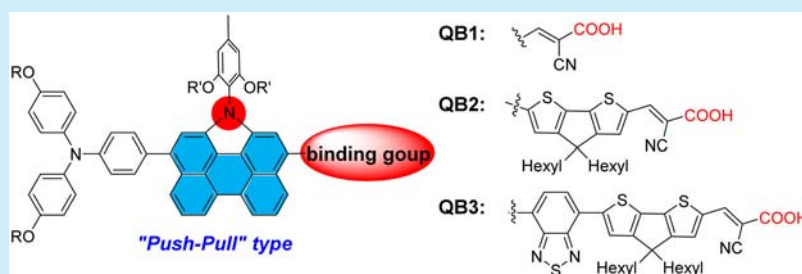


## N-Annulated Perylene-Based Push–Pull-Type Sensitizers

Qingbiao Qi,<sup>†,||</sup> Xingzhu Wang,<sup>‡,||</sup> Li Fan,<sup>‡</sup> Bin Zheng,<sup>§</sup> Wangdong Zeng,<sup>†</sup> Jie Luo,<sup>⊥</sup> Kuo-Wei Huang,<sup>§</sup> Qing Wang,<sup>\*,‡</sup> and Jishan Wu<sup>\*,†,⊥</sup><sup>†</sup>Department of Chemistry, National University of Singapore, 3 Science Drive 3, Singapore, 117543<sup>‡</sup>Department of Materials Science and Engineering, NUSNNI-NanoCore, National University of Singapore, 9 Engineering Drive 1, Singapore, 117576<sup>§</sup>KAUST Catalysis Center and Division of Physical Sciences & Engineering, King Abdullah University of Science and Technology, Thuwal 23955-6900, Saudi Arabia<sup>⊥</sup>Institute of Materials Research and Engineering, A\*STAR, 3 Research Link, Singapore, 117602

## Supporting Information



**ABSTRACT:** Alkoxy-wrapped N-annulated perylene (NP) was synthesized and used as a rigid and coplanar  $\pi$ -linker for three push–pull type metal-free sensitizers **QB1–QB3**. Their optical and electrochemical properties were tuned by varying the structure of acceptor. These new dyes were applied in Co(II)/(III) based dye-sensitized solar cells, and power conversion efficiency up to 6.95% was achieved, indicating that NP could be used as a new building block for the design of high-performance sensitizers in the future.

Design and synthesis of stable organic dyes with appropriate energy level alignment and large light-harvesting capability was the key to achieving high-performance dye-sensitized solar cells (DSCs).<sup>1</sup> In recent years, various types of organic dyes with donor– $\pi$ –acceptor structure have been investigated.<sup>2</sup> Among them, porphyrin-based push–pull-type sensitizers have demonstrated superior performance in comparison to other metal-free organic dyes.<sup>3</sup> However, the tedious synthesis makes it very hard to apply this kind of dye in practical applications.

Therefore, we started to look for a good replacement of porphyrin. Perylene could be a suitable candidate as it has an intense absorption band around 410 nm which is close to the Soret band of porphyrin. In addition, perylene-based dyes have shown excellent photophysical properties such as a high extinction coefficient, a high fluorescence quantum yield, and outstanding chemical, thermal, and photochemical stability.<sup>4</sup> In fact, perylene-based dyes have been successfully used for both organic photovoltaics<sup>5</sup> and DSCs.<sup>6</sup> However, most of them exhibited relatively low overall power conversion efficiencies and were limited to perylene anhydride and perylene imide with modification at bay position to improve solubility and suppress aggregation.

Our attention was then shifted to a new perylene derivative, the so-called N-annulated perylene (NP), in which a nitrogen

atom is annulated at the bay position.<sup>7</sup> Compared with the parent perylene, regioselective functionalization (e.g., bromination) can be conducted at the *peri*-positions near the amine side,<sup>8</sup> which opens the opportunities to generate push–pull-type sensitizers by using NP as a new rigid and coplanar  $\pi$ -linker (Figure 1). In addition, flexible alkyl chains or bulky groups can be readily introduced to the amine site, which can significantly improve the solubility and suppress dye aggregation. Moreover, NP itself has good light-harvesting ability and can also serve as an electron donor. In fact, our group recently demonstrated that NP-substituted porphyrins showed largely improved light harvesting in near-infrared region, and power conversion efficiency ( $\eta$ ) higher than 10% was achieved in Co(II)/(III) based DSCs.<sup>9</sup>

In this context, three NP-based push–pull sensitizers **QB1–QB3** (Figure 1) were synthesized and tested in DSCs in this work. The design is based on the following considerations: (1) NP shows strong absorption in visible range ( $\lambda_{\text{abs}}^{\text{max}} = 413 \text{ nm}$ ) with high extinction coefficient and high fluorescence quantum yield,<sup>8</sup> which will be good for light harvesting; (2) a bulky *o*-alkoxy-substituted phenyl group rather than flexible alkyl chain was chosen to suppress the problematic dye aggregation as well

Received: December 29, 2014

Published: January 27, 2015

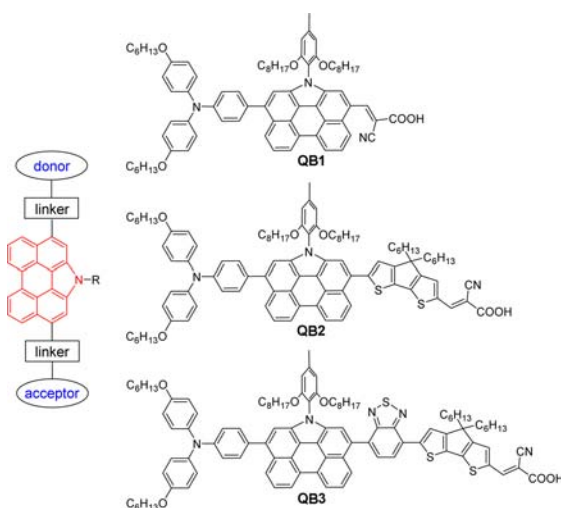


**Figure 1.** Molecular design and structures of NP-based sensitizers **QB1–QB3**.

as to ensure sufficient solubility;<sup>10</sup> (3) triphenylamine (TPA) was chosen as the electron-donating donor, while cyanoacetic acid (CAA) was chosen as electron-acceptor/anchoring group because they have been proved to be efficient for many metal-free sensitizers;<sup>2</sup> (4) for **QB2**, a 4,4-dihexyl-4*H*-cyclopenta[2,1-*b*:3,4-*b'*]dithiophene (CPDT) unit was inserted between NP and CAA in **QB1** in order to extend  $\pi$ -conjugation; (5) for **QB3**, an electron-deficient benzothiadiazole (BT) moiety was inserted between the NP and the CPDT unit in **QB2** to facilitate intramolecular charge separation and to tailor the light-harvesting property.

The synthesis commenced with the *N*-arylation of the parent NP **1**<sup>7,8</sup> with the 2,6-bis(octyloxy)-1-iodobenzene (**2**) (see synthesis in the Supporting Information) in the presence of Cu and K<sub>2</sub>CO<sub>3</sub> to give the key compound **3** (Scheme 1). Regioselective bromination of **3** with 2 equiv of *N*-bromosuccinimide (NBS) at room temperature gave the dibrominated NP **4** in 90% yield. The NP monoaldehyde **5** was then prepared by the monolithiation of **4** followed by reaction with anhydrous DMF. Suzuki coupling of compound **5** with 4,4,5,5-tetramethyl-2-[4-[*N,N*-bis(4-hexyloxyphenyl)amino]phenyl]-1,3,2-dioxaborolane (**6**)<sup>11</sup> generated the NP aldehyde **7** and subsequent Knoevenagel condensation with cyanoacetic acid in the presence of piperidine afforded the target compound **QB1** in 89% yield over two steps. Suzuki coupling between **4** and **6** gave the monobromo-NP **8**, and then the NP monoboronic ester **9** as another key intermediate was prepared by Miyaura borylation reaction from **8**. Suzuki coupling between **9** with the monobromo-CPDT **10**<sup>11</sup> or CPDT–BT **11**<sup>12</sup> gave the aldehydes **12** and **13**, respectively, and similar Knoevenagel condensation with cyanoacetic acid afforded the corresponding dyes **QB2** and **QB3**.

The absorption spectra of **QB1–QB3** in chloroform all exhibit a broad band at 400–700 nm region with large molecular extinction coefficient ( $\epsilon$ ), which can be attributed to the intramolecular donor–acceptor interaction (Figure 2). Time-dependent density functional theory (TD DFT) calculations at the B3LYP/6-31G\* level of theory suggest that this band is a combination of several electronic transitions dominated by HOMO  $\rightarrow$  LUMO, HOMO–1  $\rightarrow$  LUMO, HOMO  $\rightarrow$  LUMO+1 and HOMO–1  $\rightarrow$  LUMO+1 (see details in the Supporting Information). The absorption maximum was

**Scheme 1.** Synthetic Routes of **QB1–QB3**

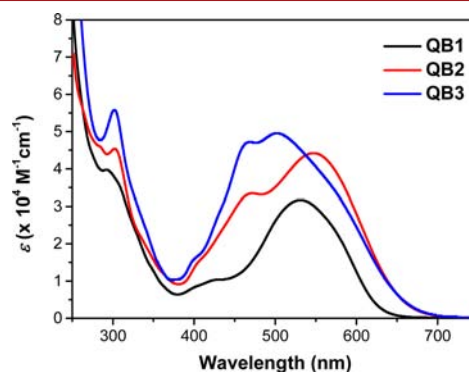
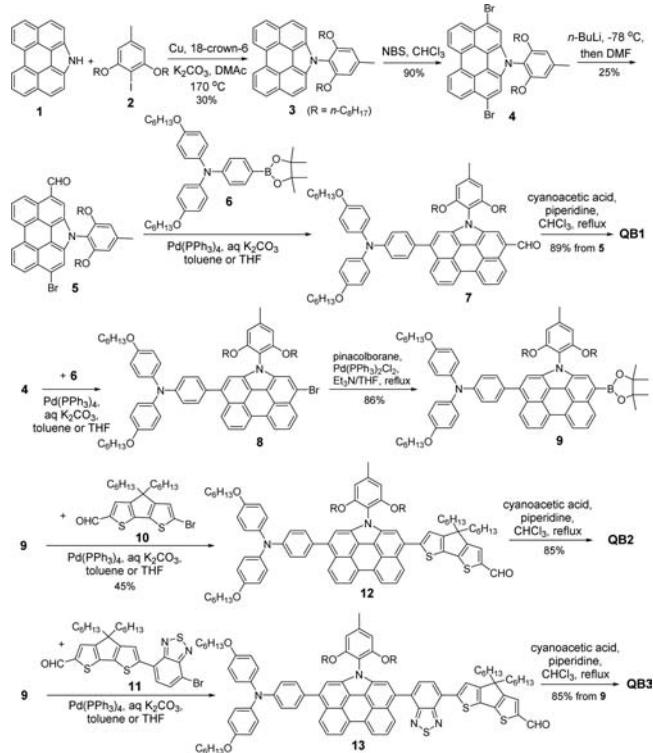


**Figure 2.** UV–vis absorption spectra of **QB1–QB3** in chloroform.

observed at 531 nm ( $\epsilon = 3.27 \times 10^4 \text{ M}^{-1} \text{ cm}^{-1}$ ) for **QB1**, 550 nm ( $\epsilon = 4.45 \times 10^4 \text{ M}^{-1} \text{ cm}^{-1}$ ) for **QB2**, and 502 nm ( $\epsilon = 4.96 \times 10^4 \text{ M}^{-1} \text{ cm}^{-1}$ ) for **QB3**. In comparison with **QB1**, the absorption maximum and absorption edge of **QB2** shift to red by 19 and 58 nm, respectively, and the spectra become more broad and intense, which can be explained by the extended  $\pi$ -conjugation after inserting of a CPDT unit. **QB3** shows similar spectral broadening and intensity enhancement, with the absorption edge shifted to the red by 60 nm. However, its absorption maximum exhibits a 29 nm blue shift, which can be explained by a larger dihedral angle (59.4°) between the NP and BT units in **QB3** than that (42.4°) between NP and CPDT units in **QB2** based on the DFT calculations (Supporting Information). The absorption spectra of three sensitizers adsorbed on transparent mesoporous TiO<sub>2</sub> films all show some blue shift presumably due to the deprotonation of –COOH group on TiO<sub>2</sub> surface (Figure S1, Supporting Information). The spectra of **QB1** and **QB2** are slightly broadened, but there is no significant change on the shape,

indicating that there is not much dye aggregation due to the introduction of bulky bisoctyloxyphenyl group to the amine site.<sup>10</sup> However, for **QB3**, the shape of its absorption spectrum is quite different and largely blue-shifted, implying possible formation of H-aggregates after inserting a BT moiety. In fact, the <sup>1</sup>H NMR spectra of **QB1** and **QB2** show sharp peaks even in concentrated solutions, but the **QB3** exhibits relatively broadened resonances (Supporting Information).

The HOMO and LUMO energy levels of **QB1–QB3** were determined to be 5.03, 4.98, 4.98 eV (HOMO) and 3.44, 3.41, 3.42 eV (LUMO), respectively, by cyclic voltammetry in CH<sub>2</sub>Cl<sub>2</sub> solution (Figure S2 and Table S1, Supporting Information). The electrochemical energy gaps were calculated accordingly to be 1.59, 1.57, and 1.56 eV, which are in agreement with the optical energy gaps. DFT (B3LYP/6-31G\*) calculations show that for **QB1**, the HOMO is delocalized along both the TPA and the NP core, while the LUMO is delocalized through the NP core and the CAA group (Figure S3, Supporting Information). **QB2** and **QB3** exhibit even more segregated HOMO and LUMO. Such a spatially well-separated orbital distribution is desirable for efficient intramolecular charge separation and fast injection of photo-excited electron into the conduction band of TiO<sub>2</sub> via the carboxylic group adsorbed on the TiO<sub>2</sub> surface.

The newly synthesized dyes **QB1–QB3** were adsorbed onto a bilayer titania film to serve as a working electrode for photovoltaic characterizations with Co(II)/(III) based electrolyte (see details in the Supporting Information).<sup>12</sup> Parts a and b of Figure 3 show the photocurrent density–voltage (*J–V*)

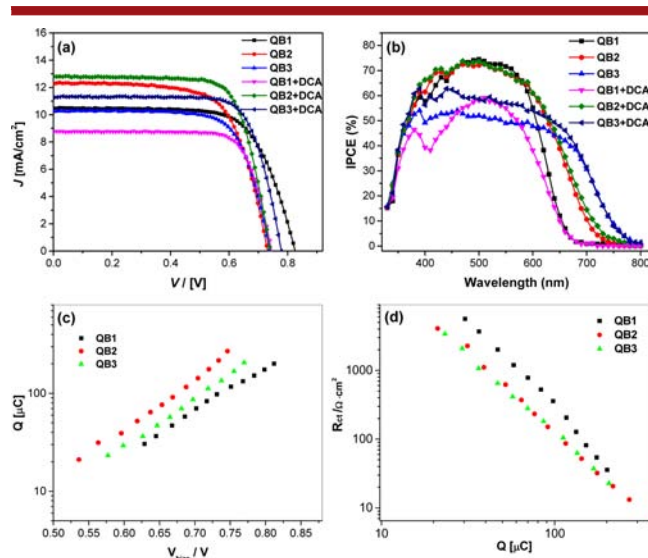


**Figure 3.** (a) Photocurrent–voltage curves and (b) IPCE action spectra of the DSCs based on **QB1–QB3** with and without coadsorbent DCA; (c) TiO<sub>2</sub> chemical capacitance (*Q*) versus bias voltage; (d) electron recombination resistance (*R<sub>ct</sub>*) versus *Q* for **QB1–QB3** cells.

characteristics and the corresponding incident photon-to-current efficiency (IPCE) action spectra under illumination of the standard AM 1.5 simulated sunlight (1 sun, 100 mW cm<sup>-2</sup>). Dyes **QB1–QB3** showed an average power conversion efficiency of 5.79%, 6.10%, and 5.46%, respectively (Table 1), which is impressive since most reported perylene based sensitizers exhibited low or moderate performance.<sup>6</sup> In particular, DSCs based on **QB1** showed large open circuit

**Table 1.** Photovoltaic Parameters of DSCs Based on **QB1–QB3** with and without Co-adsorbent DCA

| cell name        | <i>V<sub>OC</sub></i> (mV) | <i>J<sub>SC</sub></i> (mA cm <sup>-2</sup> ) | <i>ff</i> (%) | <i>η</i> (%)      |
|------------------|----------------------------|--|---------------|-------------------|
| <b>QB1</b>       | 825                        | 10.48  | 69.1          | 5.79 <sup>a</sup> |
| <b>QB2</b>       | 731                        | 12.31  | 67.8          | 6.10 <sup>a</sup> |
| <b>QB3</b>       | 739                        | 10.27  | 72.0          | 5.46 <sup>a</sup> |
| <b>QB1 + DCA</b> | 729                        | 8.76   | 74.4          | 4.76 <sup>b</sup> |
| <b>QB2 + DCA</b> | 740                        | 12.80  | 73.3          | 6.95 <sup>b</sup> |
| <b>QB3 + DCA</b> | 766                        | 11.32  | 72.6          | 6.30 <sup>b</sup> |

<sup>a</sup>The cell employed 5.3 μm TiO<sub>2</sub> transparent with 4.0 μm light scattering layers. <sup>b</sup>Coadsorbed with DCA. Dye: DCA = 1:10.

voltage (*V<sub>OC</sub>* = 0.825 V), which could be ascribed to its optimal frontier molecular orbital profile and lower HOMO energy level compared with **QB2** and **QB3**. Broad IPCE action spectra covering most of the visible region were observed for all three dyes, which is consistent with their absorption spectra. Dyes **QB1** and **QB2** showed IPCE values up to 75%, while dye **QB3** exhibited lower maximum IPCE value (~54%). The onset of IPCE action spectra is red-shifted from 663 nm for **QB1** to 715 nm for **QB2** and to 725 nm for **QB3**. As a result, **QB2** cell showed the highest short circuit current density (*J<sub>SC</sub>*) of 12.31 mA cm<sup>-2</sup> while **QB1** and **QB3** displayed smaller *J<sub>SC</sub>* values (Table 1). After coadsorption with deoxycholic acid (DCA), the power conversion efficiency dropped for the **QB1** cell (*η* = 4.76%) while slightly increased for **QB2** cell (*η* = 6.95%). Significant improvement of performance was observed for **QB3** (*η* = 6.30%) presumably due to the suppression of dye aggregation.

To further understand the dye structure–device performance relationship, electrochemical impedance measurements were conducted on the **QB1–QB3** cells under illumination and open-circuit states. As commonly understood, *V<sub>OC</sub>* is intimately correlated to the conduction band (CB) position and the charge recombination rate.<sup>13</sup> Figure 3c shows the dependence of chemical capacitance (*Q*) of the three cells on *V<sub>OC</sub>*. At a fixed bias voltage, the difference in chemical capacitance indicates the conduction band (CB) position of TiO<sub>2</sub> varies among the three cells. Apparently, the **QB1** cell presented the largest upward shift of the CB, while **QB2** the least,<sup>14</sup> largely interpreting the *V<sub>OC</sub>* difference of the cells. Figure 3d shows the recombination resistance (*R<sub>ct</sub>*) of the cells at different *Q*. At a fixed electron density, the *R<sub>ct</sub>* for **QB1** cell is larger than that for **QB2** and **QB3**, the latter two being fairly similar, which implies charge recombination is more effectively retarded by **QB1** dye. As a result, the above two factors render the highest *V<sub>OC</sub>* of **QB1** cell.

In summary, alkoxy-wrapped *N*-annulated perylene was first used as a rigid and coplanar *π*-spacer for the design of push–pull-type sensitizers. The obtained dyes **QB1–QB3** showed good light harvesting ability and superior device performance compared to many known perylene-based sensitizers. Our research suggests that NP could be a good replacement of porphyrin for the design of new high performance sensitizers in the future. Optimization of sensitizer structure by extending *π*-conjugation and/or by tuning the donor and acceptor structures is underway in our laboratories to further improve the device performance.

## ■ ASSOCIATED CONTENT

### ■ Supporting Information

Synthetic procedures and characterization data for all compounds, additional spectroscopic data, cyclic voltammograms, DFT calculation details, device fabrication, and characterizations. This material is available free of charge via the Internet at <http://pubs.acs.org>.

## ■ AUTHOR INFORMATION

### Corresponding Authors

\*E-mail: [qing.wang@nus.edu.sg](mailto:qing.wang@nus.edu.sg).

\*E-mail: [chmwuj@nus.edu.sg](mailto:chmwuj@nus.edu.sg).

### Author Contributions

<sup>||</sup>These authors contributed equally to this work.

### Notes

The authors declare no competing financial interest.

## ■ ACKNOWLEDGMENTS

J.W. and Q.W. acknowledge financial support from MOE Tier 2 grant (MOE2011-T2-2-130), A\*STAR-DST joint grant (IMRE/14-2C0239), and IMRE core funding (IMRE/13-1C0205). K.-W.H. acknowledges financial support from KAUST.

## ■ REFERENCES

- (1) (a) Oregan, B.; Grätzel, M. *Nature* **1991**, *353*, 737. (b) Imahori, H.; Umeyama, T.; Ito, S. *Acc. Chem. Res.* **2009**, *42*, 1809. (c) Hagfeldt, A.; Boschloo, G.; Sun, L.; Kloo, L.; Pettersson, H. *Chem. Rev.* **2010**, *110*, 6595. (d) Hardin, B. E.; Snaith, H. J.; McGehee, M. D. *Nat. Photonics* **2012**, *6*, 162. (e) Zhang, S.; Yang, X.; Numata, Y.; Han, L. *Energy Environ. Sci.* **2013**, *6*, 1443. (f) Ying, W.; Yang, J.; Wielopolski, M.; Moehl, T.; Moser, J.-E.; Comte, P.; Hua, J.; Zakeeruddin, S. M.; Tian, H.; Grätzel, M. *Chem. Sci.* **2014**, *5*, 206. (g) Huang, Z.; Feng, H.; Zang, X.; Iqbal, Z.; Zeng, H.; Kuang, D.; Wang, L.; Meierd, H.; Cao, D. *J. Mater. Chem. A* **2014**, *2*, 15365.
- (2) See recent reviews: (a) Mishra, A.; Fischer, M. K. R.; Bäuerle, P. *Angew. Chem., Int. Ed.* **2009**, *48*, 2474. (b) Clifford, J. N.; Martínez-Ferrero, E.; Viterisi, A.; Palomares, E. *Chem. Soc. Rev.* **2011**, *40*, 1635. (c) Liang, M.; Chen, J. *Chem. Soc. Rev.* **2013**, *42*, 3453.
- (3) (a) Li, L.-L.; Diau, E. W.-G. *Chem. Soc. Rev.* **2013**, *42*, 291. (b) Yella, A.; Lee, H.-W.; Tsao, H. N.; Yi, C.; Chandiran, A. K.; Nazeeruddin, M. K.; Diau, E.W.-G.; Yeh, C.-Y.; Zakeeruddin, S. M.; Grätzel, M. *Science* **2011**, *334*, 629. (c) Mathew, S.; Yella, A.; Gao, P.; Humphry-Baker, R.; Curchod, B. F. E.; Ashari-Astani, N.; Tavernelli, I.; Rothlisberger, U.; Nazeeruddin, M. K.; Grätzel, M. *Nat. Chem.* **2014**, *6*, 242. (d) Yella, A.; Mai, C.-L.; Zakeeruddin, S. M.; Chang, S.-N.; Hsieh, C.-H.; Yeh, C.-Y.; Grätzel, M. *Angew. Chem., Int. Ed.* **2014**, *53*, 2973. (e) Higashino, T.; Imahori, H. *Dalton Trans.* **2015**, *44*, 448.
- (4) See a recent review: Chen, L.; Li, C.; Müllen, K. *J. Mater. Chem. C* **2014**, *2*, 1938.
- (5) (a) Schmidt-Mende, L.; Fechtenkötter, A.; Müllen, K.; Moons, E.; Friend, R. H.; MacKenzie, J. D. *Science* **2001**, *293*, 1119. (b) Cremer, J.; Mena-Osteritz, E. M.; Pschierer, N. G.; Müllen, K.; Bauerle, P. *Org. Biomol. Chem.* **2005**, *3*, 985. (c) Zhan, X. W.; Tan, Z. A.; Domercq, B.; An, Z. S.; Zhang, X.; Barlow, S.; Li, Y. F.; Zhu, D. B.; Kippelen, B.; Marder, S. R. *J. Am. Chem. Soc.* **2007**, *129*, 7246. (d) Sharma, G. D.; Suresh, P.; Mikroyannidis, J. A.; Stylianakis, M. M. *J. Mater. Chem.* **2010**, *20*, 561.
- (6) (a) Ferrere, S.; Zaban, A.; Gregg, B. A. *J. Phys. Chem. B* **1997**, *101*, 4490. (b) Edvinsson, T.; Li, C.; Pschierer, N.; Schoneboom, J.; Eickemeyer, F.; Sens, R.; Boschloo, G.; Herrmann, A.; Müllen, K.; Hagfeldt, A. *J. Phys. Chem. C* **2007**, *111*, 15137. (c) Shibano, Y.; Umeyama, T.; Matano, Y.; Imahori, H. *Org. Lett.* **2007**, *9*, 1971. (d) Li, C.; Yum, J.-H.; Moon, S.-J.; Herrmann, A.; Eickemeyer, F.; Pschierer, N.

G.; Erk, P.; Schöneboom, J.; Müllen, K.; Grätzel, M.; Nazeeruddin, M. K. *ChemSusChem* **2008**, *1*, 615. (e) Li, C.; Liu, Z. H.; Schoneboom, J.; Eickemeyer, F.; Pschierer, N. G.; Erk, P.; Herrmann, A.; Müllen, K. *J. Mater. Chem.* **2009**, *19*, 5405. (f) Imahori, H.; Mathew, S. *J. Mater. Chem.* **2011**, *21*, 7166. (g) Jiao, C.; Zu, N.; Huang, K.-W.; Wang, P.; Wu, J. *Org. Lett.* **2011**, *13*, 3652. (h) Li, C.; Wonneberger, H. *Adv. Mater.* **2012**, *24*, 613. (i) Yao, Z.; Yan, C.; Zhang, M.; Li, R.; Cai, Y.; Wang, P. *Adv. Energy Mater.* **2014**, *4*, 1400244.

(7) Looker, J. J. *J. Org. Chem.* **1972**, *37*, 3379.

(8) (a) Li, Y.; Wang, Z. *Org. Lett.* **2009**, *11*, 1385. (b) Jiao, C.; Huang, K.-W.; Luo, J.; Zhang, K.; Chi, C.; Wu, J. *Org. Lett.* **2009**, *11*, 4508. (c) Li, Y.; Gao, J.; Motta, S. D.; Negri, F.; Wang, Z. *J. Am. Chem. Soc.* **2010**, *132*, 4208. (d) Jiao, C.; Huang, K.-W.; Guan, Z.; Xu, Q.-H.; Wu, J. *Org. Lett.* **2010**, *12*, 4046. (e) Jiao, C.; Huang, K.-W.; Wu, J. *Org. Lett.* **2011**, *13*, 632. (f) Zeng, Z.; Ishida, M.; Zafra, J. L.; Zhu, X.; Sung, Y. M.; Bao, N.; Webster, R. D.; Lee, B. S.; Li, R.-W.; Zeng, W.; Li, Y.; Chi, C.; Navarrete, J. T. L.; Ding, J.; Casado, J.; Kim, D.; Wu, J. *J. Am. Chem. Soc.* **2013**, *135*, 6363. (g) Zeng, Z.; Lee, S.; Zafra, J. L.; Ishida, M.; Zhu, X.; Sun, Z.; Ni, Y.; Webster, R. D.; Li, R.-W.; López Navarrete, J. L.; Chi, C.; Ding, J.; Casado, J.; Kim, D.; Wu, J. *Angew. Chem., Int. Ed.* **2013**, *52*, 8561.

(9) Luo, J.; Xu, M.; Li, R.; Huang, K.-W.; Jiang, C.; Qi, Q.; Zeng, W.; Zhang, J.; Chi, C.; Wang, P.; Wu, J. *J. Am. Chem. Soc.* **2014**, *136*, 265.

(10) (a) Lee, C. Y.; She, C. X.; Jeong, N. C.; Hupp, J. T. *Chem. Commun.* **2010**, *46*, 6090. (b) Chang, Y. C.; Wang, C. L.; Pan, T. Y.; Hong, S. H.; Lan, C. M.; Kuo, H. H.; Lo, C. F.; Hsu, H. Y.; Lin, C. Y.; Diau, E. W.-G. *Chem. Commun.* **2011**, *47*, 8910. (c) Wang, C.-L.; Lan, C.-M.; Hong, S.-H.; Wang, Y.-F.; Pan, T.-Y.; Chang, C.-W.; Kuo, H.-H.; Kuo, M.-Y.; Diau, E. W.-G.; Lin, C.-Y. *Energy Environ. Sci.* **2012**, *5*, 6933. (d) Ripolles-Sanchis, T.; Guo, B. C.; Wu, H. P.; Pan, T. Y.; Lee, H. W.; Raga, S. R.; Fabregat-Santiago, F.; Bisquert, J.; Yeh, C. Y.; Diau, E. W.-G. *Chem. Commun.* **2012**, *48*, 4368.

(11) Li, R. Z.; Liu, J. Y.; Cai, N.; Zhang, M.; Wang, P. *J. Phys. Chem. B* **2010**, *114*, 4461.

(12) Wang, X. Z.; Yang, J.; Yu, H.; Li, F.; Fan, L.; Sun, W.; Liu, Y.; Koh, Z. Y.; Pan, J. H.; Yim, W.-L.; Yan, L.; Wang, Q. *Chem. Commun.* **2014**, *50*, 3965.

(13) (a) Marinado, T.; Nonomura, K.; Nissfolk, J.; Karlsson, M. K.; Hagberg, D. P.; Sun, L.; Mori, S.; Hagfeldt, A. *Langmuir* **2010**, *26*, 2592. (b) Ronca, E.; Pastore, M.; Belpassi, L.; Tarantelli, F.; De Angelis, F. *Energy Environ. Sci.* **2013**, *6*, 183.

(14) Kopidakis, N.; Neale, N. R.; Frank, A. J. *J. Phys. Chem. B* **2006**, *110*, 12485.